JOURNAL OF APPLIED ELECTROCHEMISTRY 20 (1990) 855–863

Leaching of Raney nickel composite-coated electrodes

Y. CHOQUETTE, L. BROSSARD

Institut de recherche d'Hydro-Québec (IREQ), 1800 montéee Ste-Julie, Varennes, Québec, Canada J3X 1S1

H. MÉNARD

Département de chimie, Université de Sherbrooke, Sherbrooke, Québec, J1K 2R1 Canada

Received 19 September 1989; revised 9 November 1989

The changes in the morphology and the composition of Raney Ni composite-coated electrodes was investigated during leaching in concentrated NaOH aqueous solutions. The rate of hydrogen generated during leaching is increased by stirring the solution, raising the temperature and increasing the NaOH concentration to 6.09 M. The depletion of Al from the Raney Ni particles results in phase transformations and the metal/solution interfacial area increases with time. It is suggested that the electrodeposited nickel has a dominant influence on the hydrogen discharge since the electrocatalytic activity is practically independent of the leaching time.

1. Introduction

Raney nickel, one of the most active electrocatalysts for hydrogen electrodes, is used extensively as a cathode material for electrolytic hydrogen production [1, 2] and, also, for hydrogenation processes. The electrocatalytic activity of Raney nickel is known to depend on the nature and distribution of the different phases present in the starting alloy [3–10] as well as on the leaching process [5, 8, 9, 11] but it can also be changed by the doping effect [11–15]. The electrocatalytic activity is generally related to the surface coverage by adsorbed hydrogen on the catalyst [16–21].

A composite-coating technique has been reported recently as a cost-effective way to produce Raney Ni composite-coated (RNCC) electrodes [22]. These RNCC electrodes achieve low hydrogen overpotentials and are less expensive than those obtained by other techniques [23, 24]. The preparation method begins with the dispersion of pulverized Raney Ni alloy in a nickel plating bath. During the plating process, Raney Ni alloy particles are codeposited on the cathode and covered with the nickel which binds them together or to the substrate [22]. Once coated, the electrodes are activated by immersing them in a concentrated NaOH solution. A few authors report that the leaching process of Raney Ni particles can be achieved in acid media [25] but most experiments have been carried out in alkaline solution [5, 6, 8, 9, 12, 26–28].

This paper studies the nature of the changes in the RNCC electrode during leaching. The influence of the electrode morphology and composition on the hydrogen evolution reaction (HER) during cathodic polarization is also investigated together with the influence of parameters such as the NaOH concentration, temperature and solution agitation on the leaching process. The following techniques are used: scanning electron microscopy (SEM), X-ray powder diffraction (XRPD), electron probe X-ray microanalysis (EPMA), energy dispersive X-ray microanalysis (EDX), inductively coupled plasma atomic emission spectroscopy (ICAP), cyclic voltammetry (CV) and galvanostatic polarization.

2. Experimental details

2.1. *Electrode material*

The RNCC electrodes were prepared using the technique and apparatus described in detail in the literature [22]. The apparent surface area of each cathode was $\sim 1\,cm^2$ ($\sim 0.7\,cm \times \sim 0.7\,cm$). After electrodeposition of approximately $16.4\,mg\,cm^{-2}$ nickel, the electrode was immediately removed from the plating bath, well rinsed with triply-distilled water and dried. The amount of codeposited NiAl (50/50 % wt) particles before leaching was typically $15–18\,mg\,cm^{-2}$ for a particle size of $\leqslant 38\,\mu m$. In this case, the ratio of the weight of accumulated material (r_a) was $\sim 48–52$ % wt. The relative phase component of the NiAl alloy (~ 79 % wt Ni_2Al_3 and ~ 19 % wt $NiAl_3$) was determined by XRPD semi-quantitative analysis. The electrode was stored in a dry nitrogen atmosphere before immersion in the leaching cell or electrochemical cell.

2.2. *Chemical activation*

The leaching solution, $0.4\,dm^3$ of aqueous NaOH (from 0.51 M to 9.14 M) was saturated in hydrogen by hydrogen bubbling before the electrode was immersed. The temperature of the quiescent, that is not mechanically agitated, leaching solution was maintained constant (between 25° C and 75° C) using a water jacket. The hydrogen evolved during leaching was collected and measured volumetrically as a func-

0021-891X/90 $03.00 + .12

tion of time from the displacement of water contained in a graduated glass tube. The open-circuit potential versus the saturated calomel reference electrode (SCE) was also recorded against time with a 1286 Solartron Electrochemical Interface controlled by a HP 9000 computer. The leaching time was varied up to a maximum of 92 h, after which the electrode was rinsed with triply-distilled water and immersed for ~2 h in distilled water saturated with dissolved oxygen to render the material non-pyrophoric. The electrode was stored under a dry nitrogen atmosphere before spectroscopic examination.

2.3. *Water electrolysis*

A conventional electrochemical cell of polysulphone was used with an RNCC electrode, one Ni counter-electrode with a geometric surface area of ~100 cm^2, and a Hg/HgO/KOH 30 % wt reference electrode. The experimental procedure is described in detail in the literature [29], the only significant differences here being that the electrolyte was 1.04 M NaOH solution (BDH Chemicals) at 25° C and that the working electrode was not polished before immersion but placed directly in the electrochemical cell where leaching was performed for a given time. After leaching, a constant cathodic current of 500 mA cm^{-2} was applied for 30 min, with the result that the variation in the hydrogen overpotential with time was negligible, that is less than 1 mV min^{-1}. The current density was then varied galvanostatically from 500 mA cm^{-2} to ~1 mA cm^{-2} and the corresponding Tafel parameters, that is the Tafel slope b and the exchange-current density i_0, were calculated after correction for the ohmic drop; the solution resistance was determined by impedance spectroscopy at each current density. The A.C. potential superimposed was ~10 mV peak to peak at 1000 Hz.

In another set of experiments, cyclic voltammetry was carried out immediately after leaching in the electrochemical cell (0.8 dm^3 of 1.04 M NaOH solution at 25° C). The electrode was swept from 0 V_{rhe} (−0.840 V with respect to Hg/HgO/KOH 30 % wt) to 1.040 V_{rhe} (0.200 V with respect to Hg/HgO/KOH 30 % wt) at a scan rate of 20 mV s^{-1}.

3. Results

A typical curve of the open-circuit potential (η_{oc}) against log time for a RNCC electrode material leached in 1.04 M NaOH solution at 25° C is presented in Fig. 1. The curve may be arbitrarily divided into four regions. In region I, the time dependence of η_{oc} is negligible and the length of the plateau is called the incubation time (t_{inc}). In regions II and III, a significant decrease in η_{oc} with log time is observed: slopes $d(\eta_{oc})/d(\log(t))$ are 148 and 83 mV per decade respectively. The fourth region is characterized by η_{oc} being anodic with respect to the reversible potential for the HER. It should be pointed out that the experimental values of η_{oc} in regions I and II may vary significantly from one sample to another even if they are leached under the same experimental conditions (insert of Fig. 1). However, after ~1000 s of leaching, all the η_{oc} against log time curves are superimposed.

The curve of Fig. 1 is also given in Fig. 2 (curve iii) where η_{oc} against log time is also illustrated for polycrystalline Al (curve i), Al powder codeposited with Ni (curve ii) and electrodeposited Ni (curve iv) electrodes. It is observed that the RNCC electrode material is more noble than aluminium but less noble than electrodeposited nickel.

During leaching, the aluminium depletion of the RNCC electrode induces physical and chemical changes in the material that are consistent with the η_{oc} against log time behaviour reported in Fig. 1; these changes can be investigated using spectroscopic techniques. Morphological changes in the surface of the RNCC electrode can be seen in the SEM pictures of Fig. 3. For leaching time 0 to 10 000 s, the aluminium dissolution is manifested by holes created in the electrode material. ICAP analysis revealed that more than 50 % wt of the aluminium originally present in the electrode dissolves. For longer times, no modification of the electrode material is evident but the aluminium dissolution continues, reaching 85–95 % wt of the total original aluminium after 18 h of immersion.

The formation of holes suggests a significant increase in the metal/solution interfacial area. Potentiodynamic traces obtained for a leaching time ranging from 35 s to 18 h and corrected for the ohmic drop

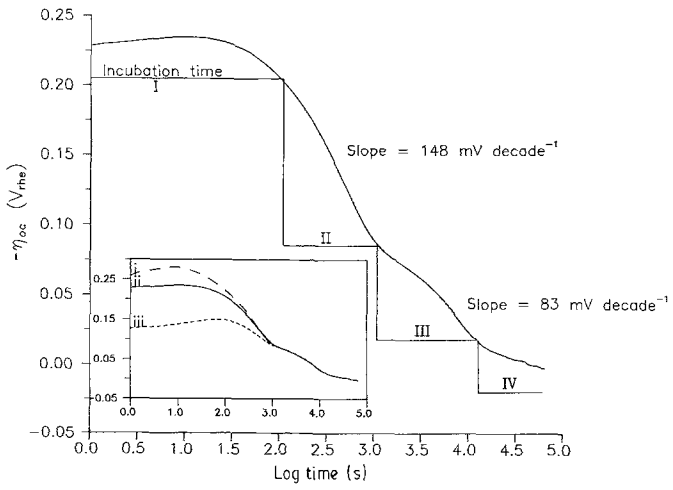

Fig. 1. Curves of η_{oc} against log time for RNCC electrodes in 1.04 M NaOH at 25° C at different leaching times. Insert: (i) 1000 s, (ii) 18 h and (iii) 10 000 s.

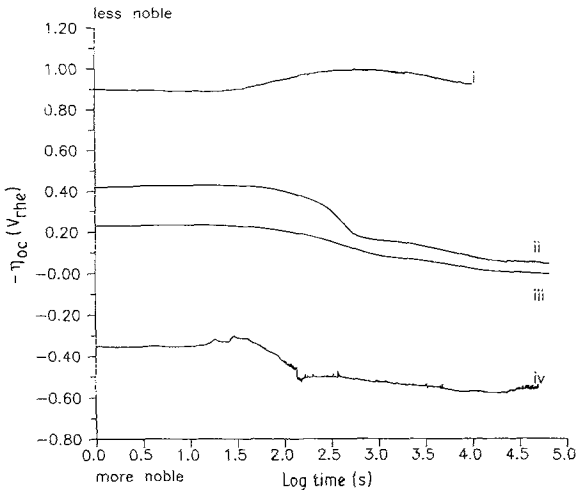

Fig. 2. Curves of η_{oc} against log time for different types of electrode immersed in 1.04 M NaOH at 25° C: (i) polycrystalline aluminium, (ii) metallic aluminium powder codeposited with nickel, (iii) RNCC electrode, (iv) electrodeposited nickel only.

are presented in Fig. 4. A very broad oxidation peak with a maximum at $\sim 0.335\ V_{rhe}$ can be distinguished; this is related to the formation of hydroxide nickel $Ni(OH)_2$ [30]. The peak height of the area below it increase considerably from 35 s to 3 160 s leaching time but only very slightly after that. This behaviour is in agreement with an increase in the metal/solution interfacial area.

The aluminium depletion rate depends on the relative amounts of the different phases, namely $NiAl_3$ and Ni_2Al_3 [3–11], present in the starting alloy. The dissolution of aluminium induces some phase transformations, which can be studied by X-ray diffraction. Six spectra are presented in Fig. 5 corresponding to RNCC electrodes leached at six different times ranging from 0 to 92 h. Most of the peaks shown were identified and analysed semi-quantitatively. Ni (~ 66 % wt), Cu (~ 7 % wt), $NiAl_3$ (~ 7 % wt) and Ni_2Al_3 (~ 18 % wt) were present on the RNCC elec-

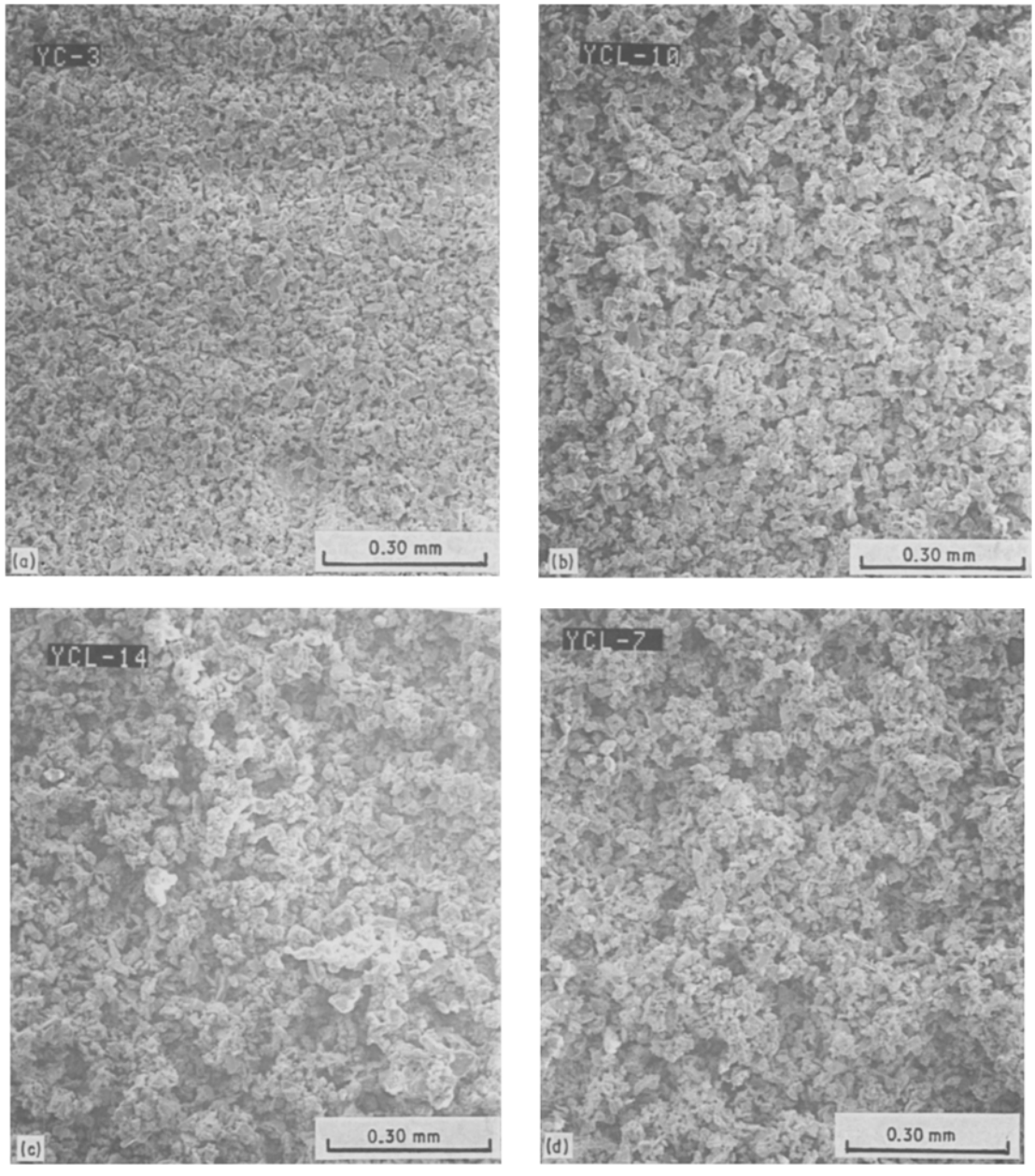

Fig. 3. Surface scanning electron micrographs (SEM) of the RNCC electrode in 1.04 M NaOH at 25° C for different leaching times: (a) 0 s, (b) 100 s, (c) 10 000 s and (d) 18 h.

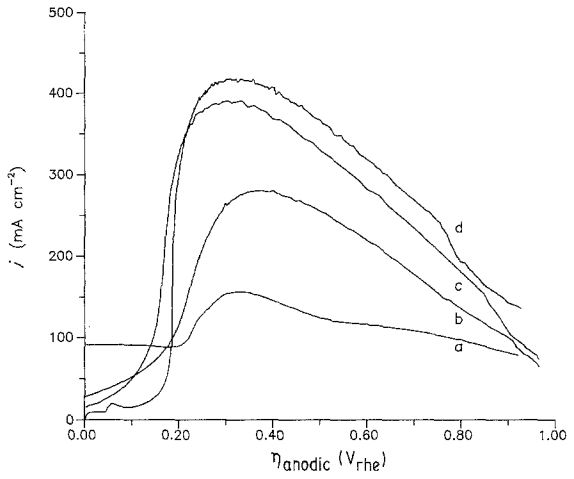

Fig. 4. Anodic portion of cyclic voltammograms for different leaching times: (a) 35 s, (b) 560 s, (c) 3160 s and (d) 18 h. Scan rate = 20 mV s^{-1}. The corresponding charge under the oxidation wave is (a) 3.78, (b) 6.67, (c) 9.55 and (d) 11.17 C cm^{-2}.

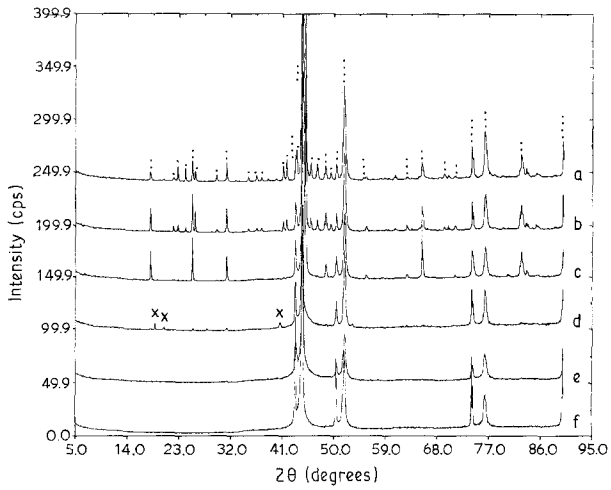

Fig. 5. Influence of leaching time on X-ray powder diffraction spectrums of the RNCC electrodes in 1.04 M NaOH at 25° C: (a) 0 s, (b) 100 s, (c) 1000 s, (d) 10 000 s, (e) 18 h and (f) 92 h. The different phases are represented by: . = $NiAl_3$, . . = Ni_2Al_3, . . . = Ni, ... = Cu and x = $Al(OH)_3$.

trode before leaching. For leaching times from 0 to 1000 s, the heights of the peaks associated with $NiAl_3$ lower with time while those corresponding to the Ni_2Al_3 increase. After 1000 s of immersion, $NiAl_3$ is not detected whereas the height of the Ni_2Al_3 peaks reaches a maximum. At this latter time, therefore, only Ni, Cu and Ni_2Al_3 are detected; it should be pointed out that the η_{oc} against log time curves (insert of Fig. 1) overlap from t = 1000 s. Peaks associated with Ni_2Al_3 become lower with time from 1000 to 10 000 s where they vanish. These phase transformations correspond to the inflection points located between regions II and III, and III and IV in Fig. 1. The spectrum d in Fig. 5 shows the presence of three small peaks that were only detected after 10 000 s of leaching and are associated with the presence of $Al(OH)_3$. At 18 and 92 h, only Ni and Cu are detected.

The morphological changes in the RNCC electrode observed during leaching suggest a possible variation in the electrocatalytic activity of the electrode towards HER. RNCC electrodes were, therefore, leached at different times and polarized cathodically. The kinetic parameters, that is Tafel slope b and the exchange-current density i_0 (illustrated in Table 1), are independent of the leaching time from 100 to 10 000 s, that is $b \sim 87$ mV per decade and $i_0 \sim 0.7$ mA cm^{-2}. Both b (110 mV per decade) and i_0 (1.51 mA cm^{-2}) increase significantly with the leaching time from 10 000 s to 18 h. The overpotential at a current density of 250 mA cm^{-2}, η_{250}, varies slightly during leaching, despite a large increase in the metal/solution interfacial area (Fig. 4).

Cross sectional views of the material were obtained for different leaching times. SEM pictures are marked * while the corresponding EPMA mappings which indicate qualitatively the presence of the chemical components, are marked ** (Fig. 6). An analysis of the porous material encapsulating each NiAl particle and covering the copper substrate showed it to be the electrodeposited nickel [22, 30]. For leaching times from 0 to 18 h, aluminium depletion was observed to enrich the nickel in the electrode. The leaching rate is not identical for all particles because some are not deeply attacked by the caustic solution after 10 000 s (Fig. 6b), which indicates that local leaching depends on the thickness and porosity of the electrodeposited nickel. However, after 18 h immersion, only traces of Al remain and cracks are observed in the particles inside the encapsulating nickel.

3.1. *Influence of temperature on the leaching process*

The η_{oc} against log time curves for RNCC electrodes leached in 1.04 M NaOH solution at 25° C to 75° C are given in Fig. 7. Leaching is seen to be largely temperature-dependent: the process is much faster at higher temperatures. This observation is also supported by the values of t_{inc}, which fall considerably with increasing temperature. The time of the first and second potential drops on these curves, that is, τ_1 and τ_2 respectively, became shorter as the temperature rose. Both shifts show the same linear log time-temperature dependence (insert in Fig. 7).

The temperature effect is also observed on the hydrogen generation rate (Fig. 8). The volume of hydrogen collected as a function of log time is approximately linear (with almost the same slope) and increases from 25° C to 55° C, although an unexpected decrease is observed at T > 55° C. Similar results were reported by Freel *et al.* [3, 4], and Choudhary

Table 1. Kinetic parameters for HER at different RNCC leaching times in 1.04 M NaOH at 25° C

Leaching time (*s*)	b (*mV decade*$^{-1}$)	i_0 (*mA cm*$^{-2}$)	η_{250} (*mV*)
100	87	0.66	225
1 000	88	0.61	231
10 000	86	0.75	217
64 800	110	1.51	244

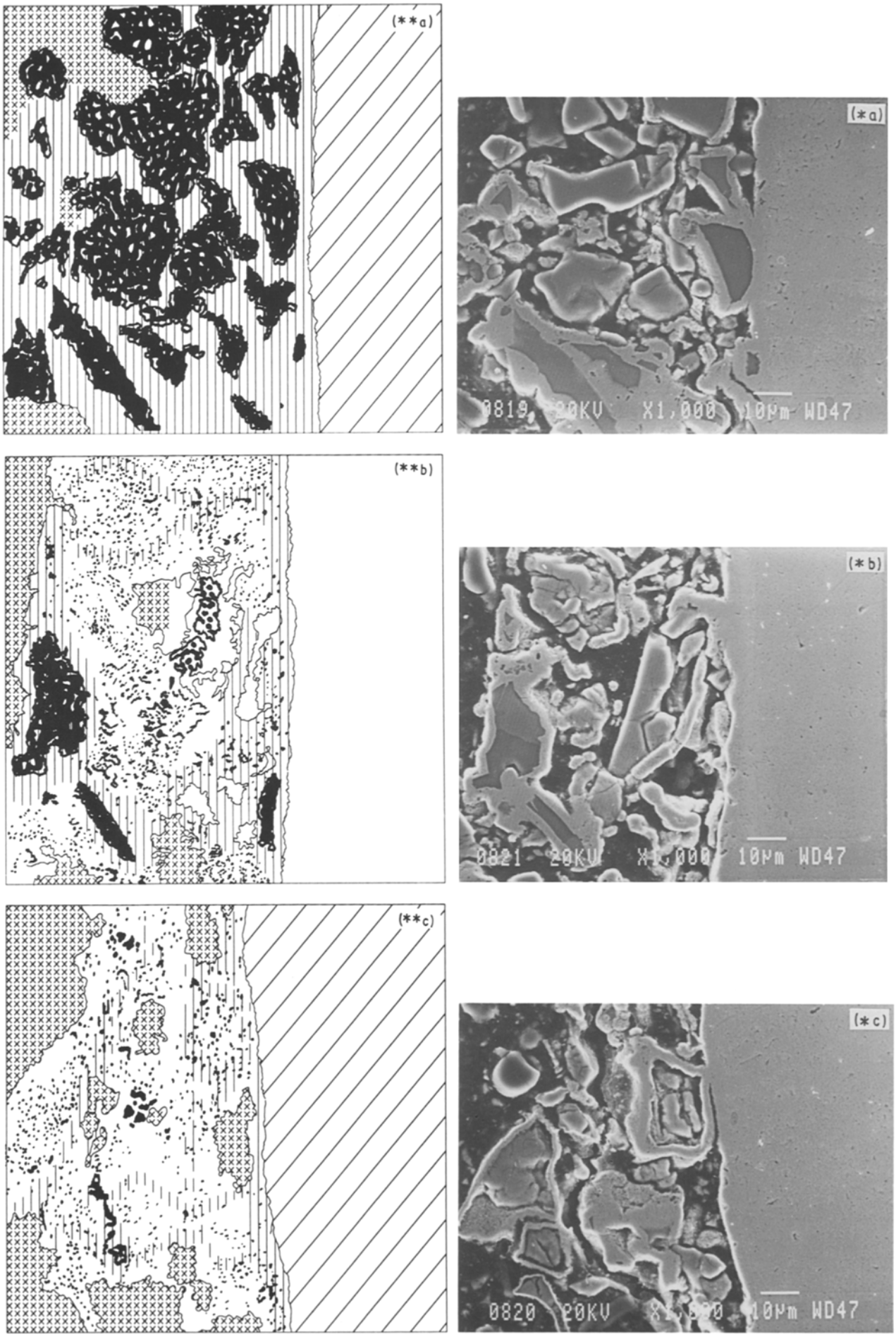

Fig. 6. Cross-section views of the RNCC electrodes leached in 1.04 M NaOH at 25° C for (a) 0 s, (b) 10 000 s and (c) 18 h. *SEM pictures and **EPMA mappings: Oblique lines = substrate; vertical lines = electrodeposited nickel; black spots = Al from NiAl particles; white spots = Ni from NiAl particles and x = resins used for the sample preparation.

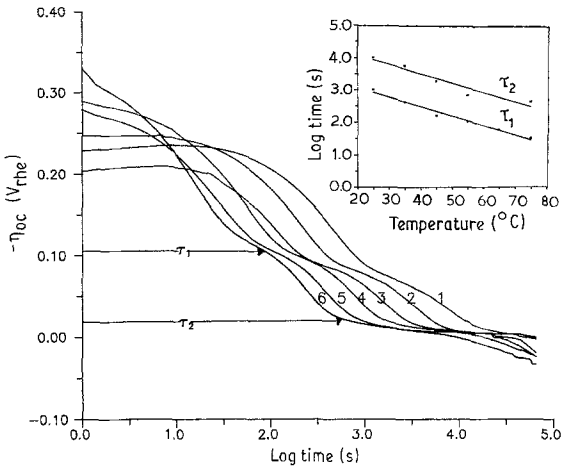

Fig. 7. Influence of temperature on the η_{oc} against log time curves for leaching of the RNCC electrode in 1.04 M NaOH: (1) 25°, (2) 35°, (3) 45°, (4) 55°, (5) 65° and (6) 75° C. Insert: temperature dependence of τ_1 and τ_2, the times of the inflection points after the first and second potential drop.

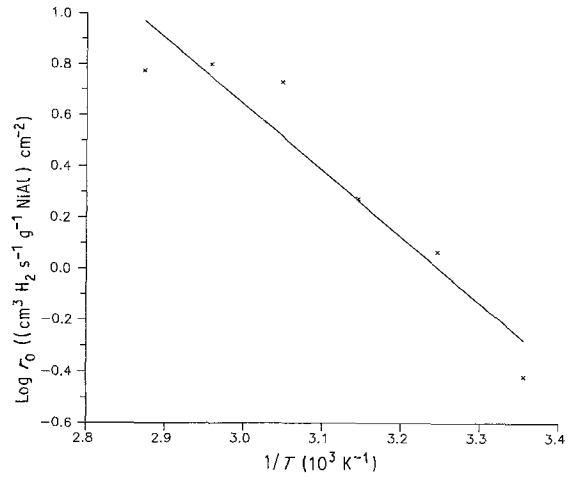

Fig. 9. Arrhenius plot considering the initial rate of the leaching process for the RNCC electrode.

and Chaudhari [27] on the dissolution of alloy powder. When the initial rate of evolved hydrogen (insert of Fig. 8), that is, log $r_{0(t\to 0)}$ is plotted against $1/T$ (Fig. 9), a linear relationship is observed and the activation energy for the leaching process may be calculated. A value of 13.6 kcal mol^{-1} is found. The empirical relationship between the volume of hydrogen collected (q) and time reported in the literature [27] namely

$$q = \alpha + \beta \log (t) \qquad (1)$$

in the case of leaching Raney Ni powder, was found to give a good fit to the kinetic data. The values of α and β for RNCC electrodes leached at different temperatures are summarized in Table II. The rate parameters for the leaching of Raney Ni powder alloy (particle size = 30–60 μm) are reported in the same table.

3.2. *Influence of stirring*

The RNCC electrodes were also leached in a quiescent and agitated (with a magnetic stirrer) 0.51 M NaOH solution at 25° C. The hydrogen volume against time curves are given in Fig. 10. The agitation results in an enlargement of time associated to the first part of the curve; in this region, the hydrogen reaction rate is maximum. However, the η_{oc} against log time curves almost superimpose for $t > t_{inc}$ whether the solution is mechanically stirred or not (insert of Fig. 10).

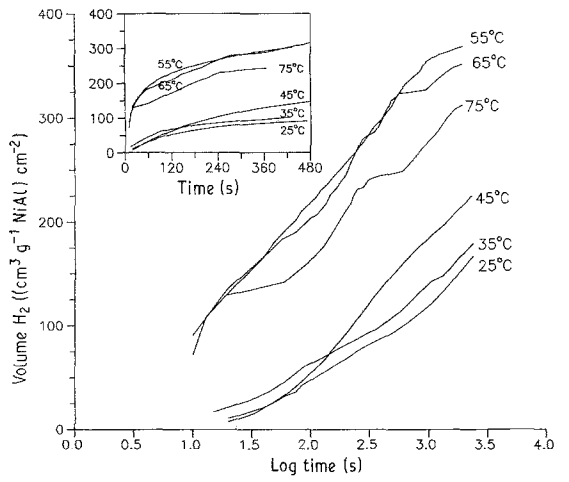

Fig. 8. Influence of temperature on the kinetics of the RNCC electrode leaching process in 1.04 M NaOH; insert: time is given on a linear scale for $t < 500$ s.

3.3. *Influence of the NaOH concentration on leaching*

The η_{oc} against log time traces for RNCC electrodes leached at 25° C at concentrations of the NaOH solution ranging from 0.51 to 9.14 M are presented in Fig. 11. Contrary to the temperature dependence, the values of τ_1 and τ_2 are not strongly influenced by the concentration. In fact, after 1000 s of leaching, all curves show approximately the same time dependence. The differences between the evolved hydrogen against time curves (insert of Fig. 11) obtained for the different concentrations are also less marked compared to the influence of the temperature. It is observed from the insert of Fig. 11 that the leaching process is faster when a 6.09 M NaOH solution is used but slows down if the concentration differs from this value. Choudhary and Chaudhari also observed this maximum for the leaching of NiAl powder [27]. Similarly, the initial rate of evolved hydrogen, r_0, reaches its maximum at 6.09 M NaOH. The curves of hydrogen volume against log time at each concentration, not presented here, were also mostly linear. In addition, when the logarithm of the r_0 values were plotted against the

Table 2. Rate parameters of Equation 1 for leaching with 1.04 M NaOH at different temperatures

Temperature (° C)	α ($cm^3\,g^{-1}$)	β*	α† ($cm^3\,g^{-1}$)	β†
25	27.9 ± 2.9	127.9 ± 1.4	62	165
35	29.0 ± 3.6	75.1 ± 1.7		
45	41.3 ± 4.1	78.6 ± 2.2		
55	189.1 ± 2.4	134.8 ± 1.0	240	150

* For a sample surface of 1 cm^2.
† From reference [27], 1.25 M NaOH.

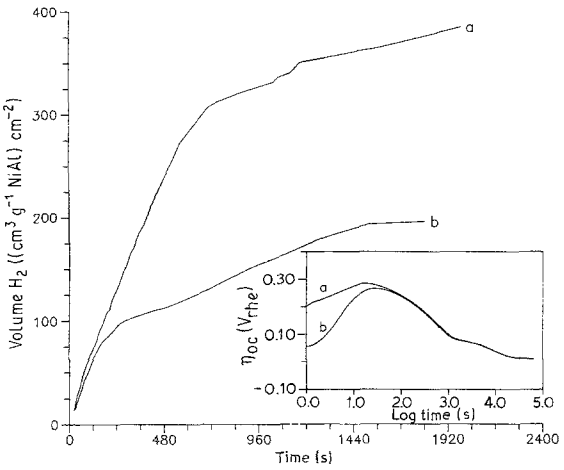

Fig. 10. Influence of the stirring of the 0.51 M NaOH solution at 25° C on the kinetics and on the η_{oc} against log time curves (insert) for the RNCC electrode leaching process: (a) agitated and (b) quiescent.

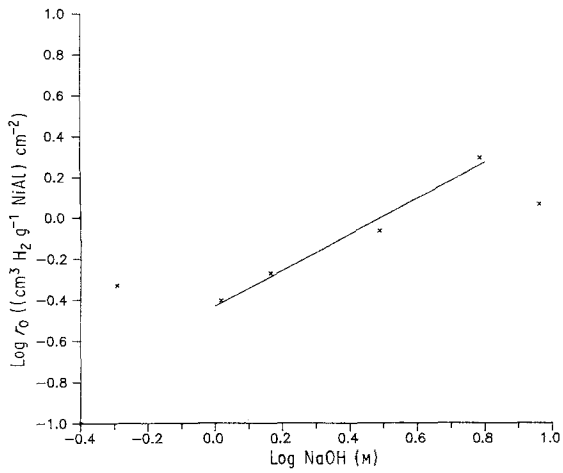

Fig. 12. Logarithm of the initial rate of evolved hydrogen (r_0) against the logarithm of NaOH concentration for the RNCC electrode leaching process at 25° C.

logarithm of the concentration (Fig. 12), a linear relationship emerged between concentrations 1.04 and 6.09 M NaOH. The experimental value of the slope is 0.8, which is close to a first-order reaction [31].

4. Discussion

Aluminium dissolution from an RNCC electrode in alkaline solution is a multistep process, as suggested by the η_{oc} against log time curve (Fig. 1). Considering the starting composition of the electrode and the XRPD spectra (Fig. 5), it is deduced that $NiAl_3$ is leached more rapidly than the other phases and is transformed into Ni_2Al_3 during the first 1000 s of immersion. During that time, the $NiAl_3$ is not detected by X-ray diffraction and is related to the inflection point following the first potential drop (Fig. 1). The X-ray penetration depends largely on the nature and structure of the sample but is generally around 5–50 μm. Since each Raney Ni particle is covered with a thick (3–4 μm) layer of electrodeposited nickel, it is possible that the X-rays do not reach the bulk of each particle. This may explain the fact that peaks corresponding to Ni are dominant in XRPD spectra and peaks associated with $NiAl_3$ and Ni_2Al_3 are small. A typical influence of the electrodeposited nickel is shown by the XRPD spectrum and EPMA mapping obtained after 10 000 s of leaching. It is observed that neither $NiAl_3$ nor Ni_2Al_3 is detected by X-ray diffraction but EPMA mapping shows that aluminium is still present in some particles, as confirmed by EDX analysis from this it is deduced that the phase changes evidenced by the XRPD spectra (Fig. 5), and the corresponding variation in η_{oc} with log time (Fig. 1) are most likely due to modifications in the composition close to the particle surface. At the end of the leaching process, η_{oc} is slightly anodic with respect to the reversible potential for the HER and hydroxide nickel is present on the electrode.

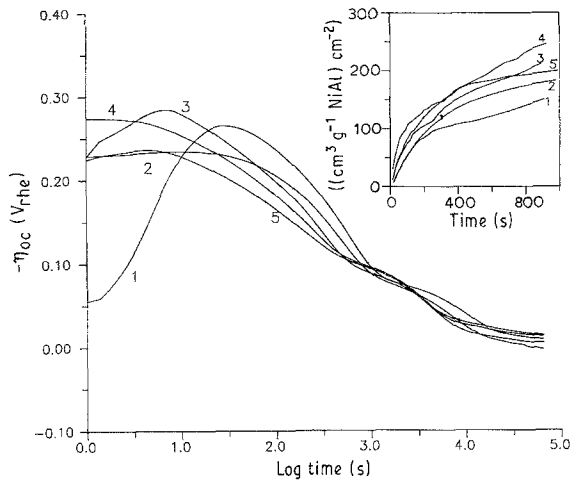

Fig. 11. Influence of the concentration of NaOH solution at 25° C on the η_{oc} against log time curves and on the kinetics (insert) of the RNCC electrodes: (1) 0.51, (2) 1.04, (3) 3.08, (4) 6.09 and (5) 9.14 M.

The electrodeposited nickel surrounding the Raney Ni particles must be porous to allow the penetration of OH^- and H_2O species which come into contact with the alloy particles. According to Birkenstock *et al.* [12], the leaching process of the NiAl powder in alkaline aqueous solutions is described by the following reactions:

$$Al + NaOH + 3H_2O \rightleftharpoons Na[Al(OH)_4] + \tfrac{3}{2}H_2 \quad (2)$$

$$Na[Al(OH)_4] + 2NaOH \rightleftharpoons Na_3[Al(OH)_6] \quad (3)$$

when the NaOH is in excess. The second reaction of the mechanism becomes:

$$Na[Al(OH)_4] \rightleftharpoons Al(OH)_3 + NaOH \quad (4)$$

where $Al(OH)_3$ tends to form hydrated alumina

$$2Al(OH)_3 \rightleftharpoons Al_2O_3 . 3H_2O \quad (5)$$

when NaOH is substoichiometric.

Since the experimental NaOH concentrations are in excess for the leaching of RNCC electrodes the presence of $Al(OH)_3$, detected by XRPD after 10 000 s of leaching, is tentatively ascribed to occlusion of the pores of the electrodeposited Ni by the solid product(s) accumulated during the dissolution process.

Penetration of the electrolyte through the electrodeposited Ni may become difficult and the concentration of the electrolyte where the reaction takes place is then substoichiometric. Alternatively, the flow of hydrogen bubbles through the porous material may also affect the electrolyte penetration rate. $Al(OH)_3$ is not detected by X-ray analysis after 18 h or even 92 h of leaching, possibly because of its transformation into an amorphous $Al_2O_3 . 3H_2O$ according to reaction (5). The presence of Al(III) species accumulated in the electrode material is in agreement with the EDX analysis, which shows the presence of Al after 18 h of leaching, that is ~ 10 wt % while the total Al dissolved in the leaching solution is always lower than the total Al originally present in the electrode material.

The marked increase in the hydrogen evolution rate during leaching from ~200 s to ~700 s in the presence of 1.04 M NaOH at 25° C when the solution is stirred (Fig. 10) suggests that external mass transfer through the liquid films surrounding the electrode material plays a significant role in controlling the rate of H_2 generated. This is consistent with the low activation-energy value found experimentally, that is 13.6 kcal mol^{-1} (Fig. 9), and with the approximately first-order reaction with respect to OH^- concentration (Fig. 12) according to reference [31]. It is relevant to note that 14 kcal mol^{-1} was found for Raney Ni powder leached in 1.25 M NaOH aqueous solution [27] but the order of reaction with respect to OH^- species is reported to be ~0.4. It is deduced that the kinetics and mechanism of the leaching process are different for the RNCC electrode and the Raney Ni particle powder. Comparison of the experimental results for the RNCC electrode with those in references [27] for Raney Ni powder could account for the fact that the stirring method is quite different in both cases. The fact that τ_1 and τ_2 are considerably lower when the temperature is raised (Fig. 7) is consistent with the low activation-energy value.

In addition, the rate parameters α and β of equation 1, which describe the amount of hydrogen generated versus time, are lower for the RNCC electrode than for the Raney Ni particle powder (Table 2). This is attributed to the need for the electrolyte and hydrogen bubbles to flow through the electrodeposited porous nickel surrounding the Raney Ni particles.

EPMA mappings show that the bulk of NiAl particles is progressively leached with time (Fig. 6) and it is deduced that the amount of Ni available during potentiodynamic oxidation increases with time (Fig. 4). Since the electrocatalytic activity towards the HER remains approximately constant with the leaching time (Table 1), the electrodeposited Ni has a dominant influence on the HER under cathodic polarization. It is suggested that hydrogen bubbles form in the pores of leached NiAl particles when the RNCC electrode is under cathodic polarization. The resulting pore blockage may reduce access to the bulk electrolyte inside the particles and the reaction proceeds mainly in the electrodeposited material. The electrocatalytic activity of the material is therefore independent on the remaining Penetration of the electrolyte through the electrodeposited Ni may become difficult and the concention [16–21] than nickel. It is also known that the RNCC electrode is more electrocatalytic towards HER than the electrodeposited nickel [22].

The rate of hydrogen generated is reported to increase up to 6.09 M NaOH and to drop from 6.09 M to 9.14 M (insert of Fig. 11) at $T = 25°$ C despite the greater activity of OH^- species at 9.14 M [32]. It is deduced that the considerable increase in the electrolyte viscosity from 6·09 M to 9.14 M [32] slows down the flow of the hydrogen bubbles through the electrode material. However, it was observed that leaching of the RNCC electrode is fastest when a 6.09 M NaOH solution is used at 70° C.

5. Conclusion

The phase transformations occurring in the RNCC electrode material during leaching are demonstrated by different techniques. The depletion of Al from the Raney Ni particles is shown to cause these phase transformations: $NiAl_3 \Rightarrow Ni_2Al_3 \Rightarrow$ porous nickel hydroxide. The rate of hydrogen generated during leaching is increased by stirring the solution, raising temperature and increasing the NaOH concentration to 6.09 M. Despite the increase in the metal/solution interfacial area with time during leaching, the electrocatalytic activity towards HER varies only slightly, suggesting that the electrodeposited nickel has a dominant effect on the hydrogen evolution reaction.

Acknowledgements

Scholarships from the National Research Council of Canada and Québec Government FCAR, financial support from Hydro-Québec are gratefully acknowledged (Y. Choquette). The authors also thank A. Joly and R. Dubuc of IREQ for the spectroscopic measurements and J. Boutin of Alcan International Limited for the EPMA mappings.

References

[1] G. T. Bowen, H. J. Davis, B. F. Henshaw, R. Lachance, R. L. Leroy and R. Renaud, *Int. J. Hydrogen Energy* **9** (1984) 59.
[2] K. Lorhberg and P. Kohl, *Electrochim. Acta* **29** (1984) 1557.
[3] J. Freel, W. J. M. Pieters and R. B. Anderson, *J. Catalysis* **16** (1970) 281.
[4] *Idem, ibid.*, **14** (1984) 247.
[5] R. Sassoulas and Y. Trambouze, *Soc. chim.* (France), 5e série (1964) 985.
[6] P. Fouilloux, G. A. Martin, A. J. Renouprez, B. Moraweck, B. Imelik et M. Piettre, *J. of Catalysis* **25** (1972) 212.
[7] C. Allibert, A. Wicker, J. Driole et E. Bonnier, *Rev. htes Temp. et Refractaires* 7 (1970) 45.
[8] A. I. Savelov and A. B. Fasman, *J. Phys. Chem.* (*Russia*) **59** (1985) 599.
[9] J. C. Klein and D. M. Hercules, *Anal. Chem.* **53** (1981) 754.
[10] F. Delanney, *Reactivity of Solids* **2** (1986) 235.
[11] S. D. Mikhailenko, A. B. Fasman, N. A. Maksinova and E. V. Leongard, *Appl. Catalysis* **12** (1984) 141.
[12] U. Birkenstock, R. Holm, B. Reinfandt and S. Storp, *J. Catalysis* **93** (1985) 55.
[13] J. C. Klein and M. Hercules, *Anal. Chem.* **56** (1984) 685.

[14] E. A. Vishnevetskii, S. D. Mikhailenko, N. A. Maksinova, A. B. Fasman, *React. Kinet. Catal. Lett.* **31** (1986) 445.
[15] N. A. Maksimova, E. A. Vishnevetskii, V. Sh. Iranov and A. B. Fasman, *Appl. Catalysis* **35** (1987) 59.
[16] J. Heiszman, K. Payer, S. Bekassy and J. Petro, *Acta Chem. Acad. Science Hung.* **T84 4** (1972) 431.
[17] A. Tungler, J. Petro, T. Mathe, J. Heiszman, S. Bekassy and S. Crusos, *ibid.* **T89 1** (1976) 31.
[18] G. L. Padyukova, G. A. Pushkareva, A. B. Fasman and K. Almashev, *Sov. Electrochim.* **22** (1986) 701.
[19] H. A. Smith, A. J. Chadwell Jr and S. S. Kirslis, *J. Phys. Chem.* **59** (1955) 820.
[20] R. J. Kokes and P. H. Emmett, *J. Am. Chem. Soc.* **81** (1959) 5032.
[21] G. L. Padyukova, G. A. Pushkareva, A. B. Fasman and B. K. Almashev, *Elektrokhimiya* **22** (1986) 747.
[22] Y. Choquette, H. Ménard and L. Brossard, *Int. J. Hydrogen Energy* **14** (1989) 637.
[23] K. Lorhberg, H. Wullenweber, J. Muller and B. Sarmond, U.S. Patent 4 278 568 (1981).
[24] A. Nidols and R. Schira, *Ext. Abstr. No. 236*, Electrochem. Soc. Meeting, Cincinnati (May 1984).
[25] K. Machida and M. Enyo, *J. Res. Inst. Catalysis* **32** (1984) 37.
[26] S. D. Robertson, J. Freel and R. B. Anderson, *J. of Catalysis* **24** (1972) 130.
[27] V. R. Choudhary and S. K. Chaudhari, *J. Chem. Tech. Biotechnol.* **33a** (1983) 339.
[28] S. D. Mikailenko, G. B. Baeva, B. F. Petrov and A. B. Fasman, *Reactivity of Solids* **2** (1987) 373.
[29] J.-Y. Huot and L. Brossard, *Int. J. Hydrogen* **12** (1987) 599.
[30] Y. Choquette, H. Ménard and L. Brossard, *Int. J. Hydrogen Energy* (in press).
[31] A. W. Adamson, 'A Textbook of Physical Chemistry', 2nd edition, Academic Press, London (1979).
[32] 'Handbook of Chemistry and Physics', CRC Press, 63rd edition (1982).